Nonequilibrium transport of polyacrylamides correlated with pore-water velocity

A Dissertation
Presented to
The Academic Faculty

by

Yuening Tang

In Partial Fulfillment
of the Requirements for the Degree
Master in the
Environmental Engineering

Georgia Institute of Technology
May/2017

NONEQUILIBRIUM TRANSPORT OF POLYACRYLAMIDES CORRELATED WITH PORE-WATER VELOCITY

Approved by:

Dr. Jian Luo, Advisor
School of Civil Engineering
Georgia Institute of Technology

Dr. Jingfeng Wang
School of Civil Engineering
Georgia Institute of Technology

Dr. Yongsheng Chen
School of Environmental Engineering
Georgia Institute of Technology

Date Approved: [April, 19th, 2017]

ACKNOWLEDGEMENTS

I cannot express enough thanks to all who have helped me during my experience at Georgia Tech. Foremost, I would like to thank my advisor, Dr. Jian Luo. He has provided me unending personal and academic guidance and taught me a great deal about both scientific research and life. I am truly grateful to have the opportunity to work with him. I would like to show gratitude for my thesis committee members, Dr. Yongsheng Chen and Dr. Jingfeng Wang who have been supportive of my research.

TABLE OF CONTENTS

LIST OF TABLES

LIST OF FIGURES

LIST OF SYMBOLS AND ABBREVIATIONS

S_{eq}	equilibrium concentration of PAM in the solid phase (mg/mg)
C	concentration in the liquid phase (mg/L)
K_L	Langmuir constant (L/mg)
$\Gamma_{\max}$	sorption capacity (mg/mg)
t	Time (min)
x	distance from the inlet (cm)
v	average pore velocity (cm/min)
D	dispersion coefficient (m^2/s)
D_H	hydrodynamic dispersion coefficient (m^2/s)
q	water flux (ml/min)
θ	effective porosity
α	mass transfer coefficient (mg/(L*min))
$D_{molecular}$	diffusion coefficient (m^2/s)
α_d	Longitudinal dispersivity (m)

SUMMARY

Transport behavior of polyacrylamides (PAMs) in chernozem was investigated through the static equilibrium sorption experiment, column tests and modeling studies. In flow-through column studies, nonequilibrium sorption behavior of PAMs was described by a nonequilibrium mass transfer model combined with a Langmuir sorption model. Langmuir sorption isotherm parameters were obtained from the static sorption experiment and dispersion coefficients and pore velocities were obtained from breakthrough curves (BTCs) of Br-. Comparing with the traditional nonequilibrium mass transfer model with a linear isotherm, the developed nonlinear model predicts asymmetric sorption and desorption behavior. More importantly, we identified a strong linear relationship between the estimated first-order mass transfer rate coefficient and the pore velocity, which relates the empirical parameter mass transfer rate coefficients to the measurable system parameter of pore velocity. Our results suggest that mass transfer may limit the subsurface transport of PAMs and the lumped mass transfer rate coefficients are linearly correlated with flow velocities. The results also indicate that this one-site Langmuir sorption model may be applied to other contaminants' transport during which the Langmuir mass transfer exists.

CHAPTER 1. INTRODUCTION

Polyacrylamides (PAMs) have been widely used in many oil fields in China for enhancing oil recovery and can be applied in erosion control and irrigation furrow [1][2]. While the benefits of using PAMs for oil exploitation are significant, its potential adverse environmental effects have attracted attention of environmental interest groups, governments, and academia.

Cationic and neutral PAMs are typically precluded from sensitive environments for their toxicities [2]. While anionic PAMs at low concentrations (e.g., 20 ppm or less) are environmentally safe [2], prolonged, large-scale applications of PAMs in oil fields may produce substantial leakage of PAMs at high concentrations that may have negative impact on soil and environment. Infiltration and runoff may further spread PAMs to deeper soils and aquifers. As a consequence, PAMs-contaminated soils have become non-arable in many regions of oil fields in China. For example over the Daqing oil field, the largest oil field in China where soil samples used in the present study were collected, more thanone hundred thousand tons of PAMs per year have been used in oil drilling over the past decades. Due to leakage of PAMs from storage, transportation, injection and oil production processes, soils in the Daqing district have been polluted and large areas of lands have become non-cultivable anymore. Polluted groundwater in these areas due to infiltration of PAMs has profound impact on local ecology.

Sojka and Entry (1999, 2000) studied the potential effect of PAM on microbial ecology and found that the accumulation of PAM in soils might reduce the active bacteria [3]. It was

also reported that PAMs may influence colloidal suspension and flocculation in soils [4][5]. Shokrollah and Abbasi (2011) found that PAMs at high concentrations were able to reduce infiltration and change physical property of sandy loam soils by decreasing saturated hydraulic conductivity during transport [6]. Given the extensive use of PAMs in China and the potential negative impact, there is an urgen need to design and implement remediation strategies to remove PAMs from contaminated groundwater and soils. For effective remediation, physical models of PAMs are needed for understanding and predicting the fate and transport of PAMs.

As PAMs degrade very slowly [7][8], and the transport in groundwater is mainly controlled by advection, dispersion and sorption processes. Equilibrium sorption behavior of PAMs has been extensively studied. Lu and Wu (2002) found that the equilibrium sorption of PAMs in soils could be described by a Langmuir isotherm and PAMs have a high sorption capacity in the soils of high clay content or low organic matter content [4]. Meadows and Williams (1989) reported that the equilibrium sorption behavior of PAMs changes with ionic strength [9]. Malik and Letey (1990) found that adsorption of PAMs was approximately constant for all soils of similar aggregate sizes [10]. However, there is limited research on nonequilibrium sorption of PAMs with groundwater flow, although it is well known that the remediation of contaminated soils and groundwater is strongly affected by nonequilibrium processes.

In this study, we aim to investigate the transport behavior of PAMs in groundwater and soil through both laboratory experiment and numerical simulation. In particular, we are interested in the sorption of PAMs under flow conditions. Specific questions to be addressed include (1) whether the sorption is equilibrium or nonequilibrium and (2) how

the sorption behavior is affected by groundwater flow. Soil samples from the Daqing oil field were packed in a column for the flow-through tracer experiment. A new transport model is developed for simulating the transport of PAMs to characterize the sorption at high concentrations. Finally, we use the model and tracer data to establish the relationship between sorption coefficients and physical transport parameters such as pore velocity and residence time.

CHAPTER 2. METHODS AND MATERIAL

2.1 Chemicals and Soil Samples

PAMs used in this study, the same as those used in oil production, were provided by the Daqing Lianhua Company (China). The molecular weight of PAMs is 3×10^6 g/mol. Various concentrations of PAM solutions, up to 1000 mg/L, were used for equilibrium sorption tests and column studies. Bromide was used as the control experiment for column studies. KBr was purchased from Damao Chemical Company (Tianjin, China). Soil samples were collected from shallow aquifers at the Daqing oil field. Physical properties of the soil measured in laboratory are summarized in Table 2.1.

Table 2.1. Physical Properties of Chernozem

Soil Type	pH	Porosity	Moisture	Organic Matter
Chernozem	7.8	0.45	2.2%	4.31%

2.2 Analytics

Concentrations of Br^- and PAM were measured by turbidity method and spectrophotometry, respectively.

2.3 Static Equilibrium Sorption

Equal volumes of PAM solutions with different concentrations, 200 mg/L, 400 mg/L, 600 mg/L, 800 mg/L and 1000 mg/L, were prepared at room temperature, 20^0C. Then 1 mg of

soil sample was added to each flask. Three samples were prepared for each concentration. Each sample was well mixed (JJ-1 electrical stirrer). After 24h, samples were centrifuged at 2200 rpm for 5 minutes and then the PAM concentration of supernatant liquid was measured based on its turbidity using Chinese standard SY/T 5329-94.

2.4 Column Studies

A plexiglass column (Height = 40 cm and Diameter = 10 cm) was packed with collected soil samples. Distilled water passed through the column first. After the column was saturated with distilled water, the outlet of the column was closed and a mixture solution of 120 mg/L KBr and 300 mg/L PAM was connected to the inlet through a pump to control the flow rate. Samples were continuously collected from the outlet to obtain the concentration breakthrough curves (BTCs). Equilibrium was reached when concentrations of Br^- and PAM reach 120 mg/L and 300 mg/L at the outlet. After an equilibrium is reached, the mixed solution was replaced with distilled water to flush the column. Samples were collected and measured continuously until concentrations of Br^- and PAMs dropped to zero. The column experiment was repeated at flow rates of 10 ml/min, 20 ml/min, 30 ml/min, 40 ml/min and 50 ml/min.

2.5 Modeling and Data Analysis

Langmuir isotherm was used to describe the static equilibrium sorption of PAMs:

$$S_{eq} = \frac{\Gamma_{\max} K_L C}{1 + K_L C} \tag{2.1}$$

where S_{eq} (mg/mg) is the equilibrium concentration of PAM in solid phase, C (mg/L) the concentration in liquid phase, K_L (L/mg) the Langmuir constant, and $\Gamma_{\max}$ (mg/mg) the sorption capacity.

A one-dimensional advection-diffusion equation was used to describe the bromide transport:

$$\frac{\partial C}{\partial t} = D_H \frac{\partial^2 C}{\partial x^2} - v\frac{\partial C}{\partial x} \tag{2.2}$$

where t (min) is time, x (cm) is the distance from the inlet, v (cm/min) the averaged pore velocity, and D_H (cm^2/min) the dispersion coefficient.

The nonequilibrium mass transfer of PAMs in the column was described by a one-dimensional advection-dispersion model:

$$\theta\frac{\partial C}{\partial t} + \rho\frac{\partial S}{\partial t} = D\frac{\partial^2 C}{\partial x^2} - q\frac{\partial C}{\partial x} \tag{2.3}$$

$$\rho\frac{\partial S}{\partial t} = \alpha(S_{eq} - S) \tag{2.4}$$

where q (cm/min) is water flux, D (cm^2/min) dispersion coefficient, θ effective porosity, ρ (mg/L) the bulk density, α [mg/(L·min)] the mass transfer coefficient, and S_{eq} (mg/mg) the equilibrium concentration of PAM in solid phase.

Most of previous models of nonequilibrium mass transfer assume linear sorption isotherm as the concentration in the liquid phase is typically low. In our study, the concentrations of

PAMs were high and approached the sorption capacity. Thus, the equilibrium concentration S_{eq} is represented by the Langmuir model, Eq. (2.1) and Eq. (2.4) becomes:

$$\rho \frac{\partial S}{\partial t} = \alpha \left(\frac{\Gamma_{\max} K_L C}{1 + K_L C} - S \right) \tag{2.5}$$

CHAPTER 3. RESULTS AND DISCUSSION

3.1 Static Sorption of PAM

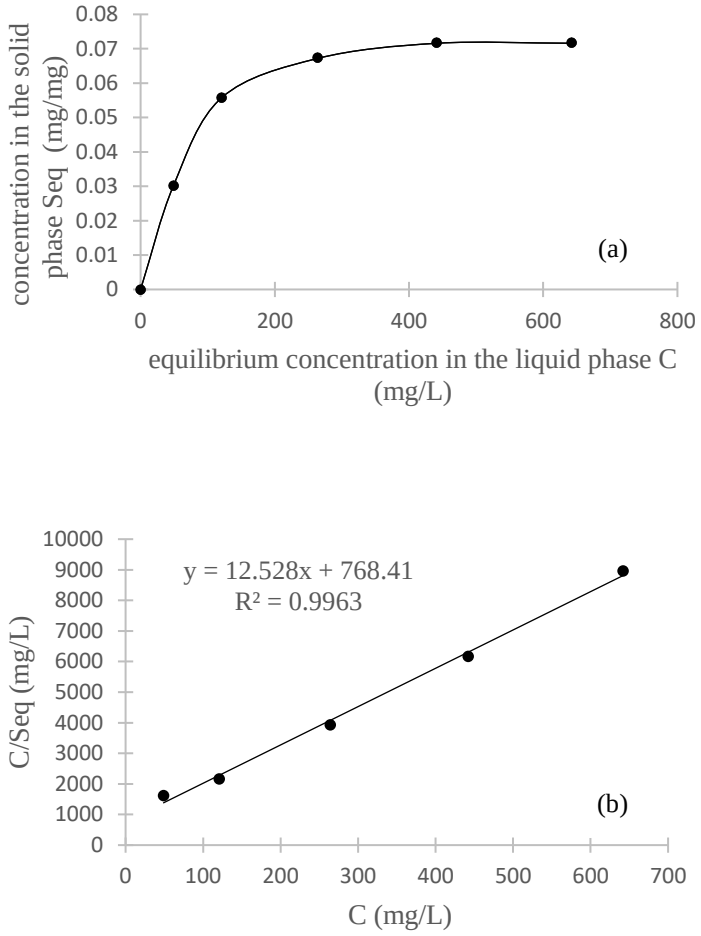

Figure 3.1. Estimation of a Langmuir sorption isotherm of PAMs

Figure 3.1 shows the estimation of a Langmuir sorption isotherm of PAMs. Figure 3.1a shows the L-type shaped sorption isotherm [4][11]. Previous studies also found that sorption isotherms of PAM were L-type in various soils [5][9][12][13]. The equilibrium concentration

of PAMs in the column experiment was 300 mg/L beyond the linear stage of Langmuir isotherm suggesting that linear mass transfer model may not be valid and a Langmuir sorption model is more suitable to describe sorption of PAM in our flow-through column experiment. Langmuir equilibrium constants K_L and $\Gamma_{\max}$ were obtained from Figure 3.1b:

$K_L = 0.0016 L/mg$, $\Gamma_{\max} = 0.08 mg/mg$

K_L and $\Gamma_{\max}$ were kept constant in the numerical simulations.

The soil used in this experiment was chernozem with high content of organic matter, which was expected to reduce PAM sorption [4]. However, PAM still had a high equilibrium concentration and its sorption capacity was higher than most pesticides and herbicides due to high molecular weight of long chain PAM molecules. The looping structure of the long chain molecules resulting from charge repulsion leads to large absorbing surface [4][14]. Therefore, PAMs can access the surface of sorbents and may be difficult to enter inter-surfaces of porous media [4] which implies that two-region (i.e., mobile-immobile) transport models may not be necessary to describe PAM transfer between the solid phase and liquid phase.

3.2 Transport of Bromide

Dispersion coefficients and mean pore velocities were estimated from breakthrough curves (BTCs) of Br^-. Measured and simulated BTCs of Br^- for various flow rates are presented in Figure 3.2.

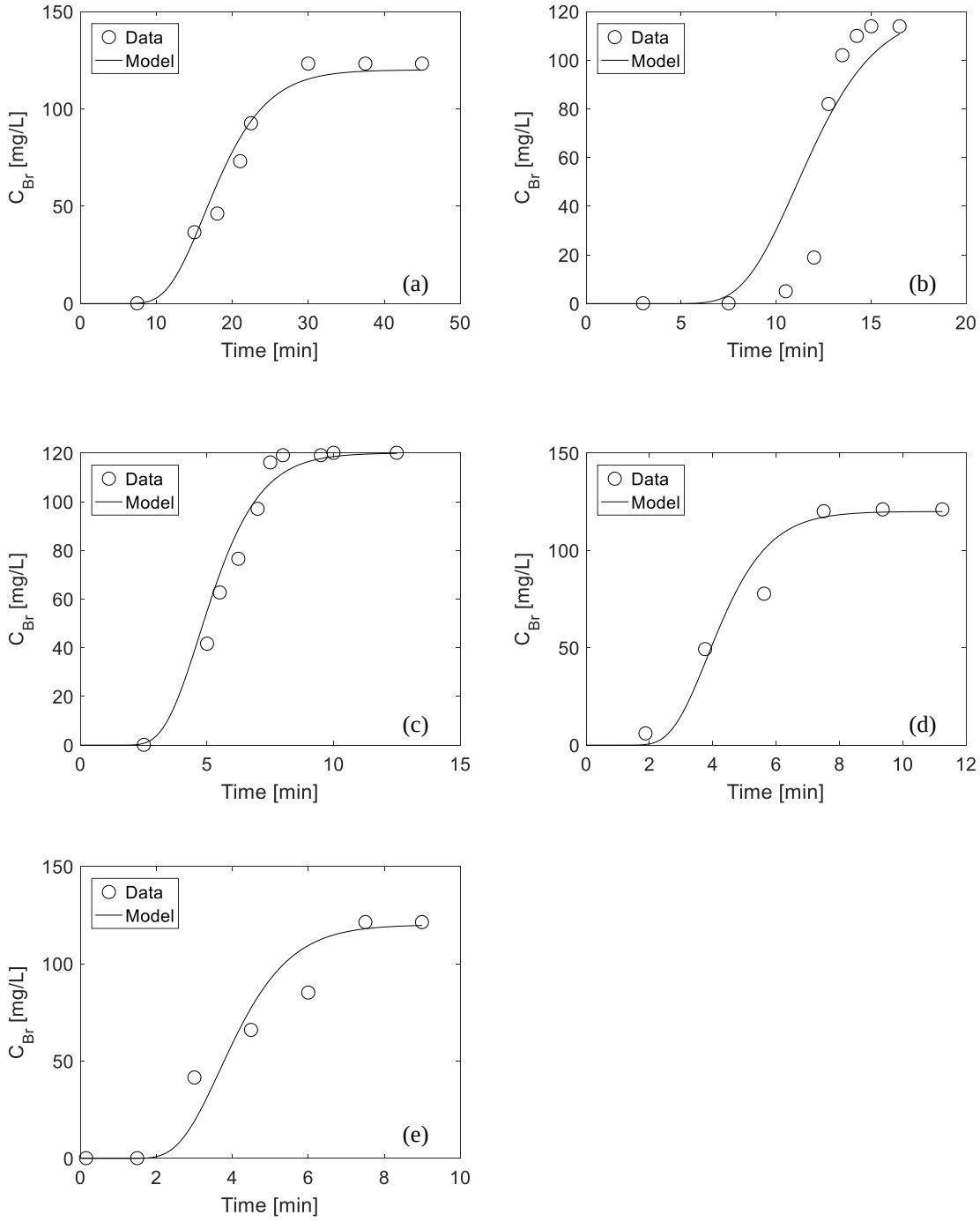

Figure 3.2. Experimental measurements and model predictions of Br^- at flow rates of (a) $Q = 10ml/\min$ (b) $Q = 20ml/\min$ (c) $Q = 30ml/\min$ (d) $Q = 40ml/\min$ (e) $Q = 50ml/\min$. Circles are experimental measurements. Lines are model predictions.

Parameters in the transport model of bromide are shown in Table 3.1. Dispersion coefficient D_H and mean pore velocity v were estimated by fitting the advection-diffusion model to measured concentrations of Br^-. Flow rate Q was controlled by a pump in the experiment.

Table 3.1. Parameters in the Model of Bromide

Q (ml/min)	v (cm/min)	D_H (cm2/min)	θ
10	0.538	0.242	0.237
20	0.828	0.242	0.308
30	1.856	0.834	0.206
40	2.278	1.025	0.224
50	2.372	1.068	0.268

In general, the hydrodynamic dispersion coefficient may be expressed by:

$$D_H = D_{molecular} + \alpha_d \cdot v \tag{3.1}$$

$D_{molecular}$ is the molecular diffusion coefficient of bromide in the porous medium, and α_d is the longitudinal dispersivity.

Molecular diffusion coefficient of Bromide, 2×10^{-9} m^2/s [15], is much smaller than D_H. Therefore, the longitudinal dispersivity α_d may be estimated from the linear regression equation of D_H and v shown in Figure 3.3.

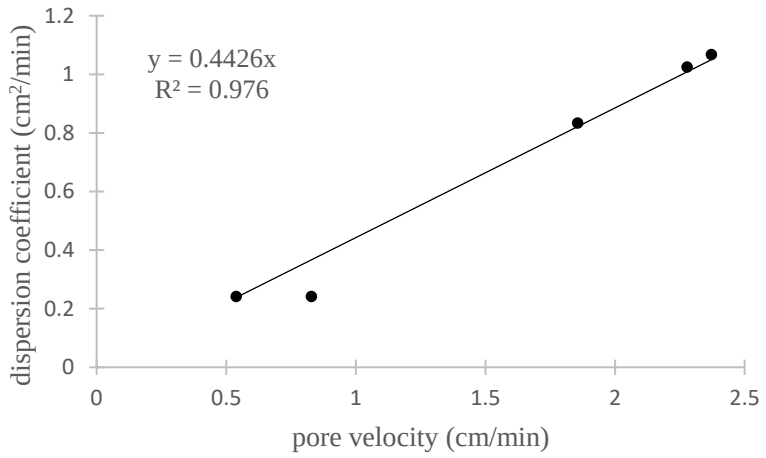

Figure 3.3. Linear Regression Equation of D_H and v

Dispersivity α_d, 0.0044 m in this experiment, is close to those reported previously [16][17][18][19]. α_d characterizes local heterogeneity of porous media [13][16] causing pore-scale velocity variations. Pore-scale velocities may fluctuate substantially due to strong local heterogeneity characterized by variable pore sizes and tortuous flow paths. Low α_d corresponding to weak local heterogeneity justifies the assumption of macroscopical homogeneity and validity of 1-D advection-diffusion model. The longitudinal dispersion coefficient and mean pore velocity estimated above were used in the numerical simulation of PAM transport discussed below.

3.3 Nonequilibrium Sorption and Desorption of PAM

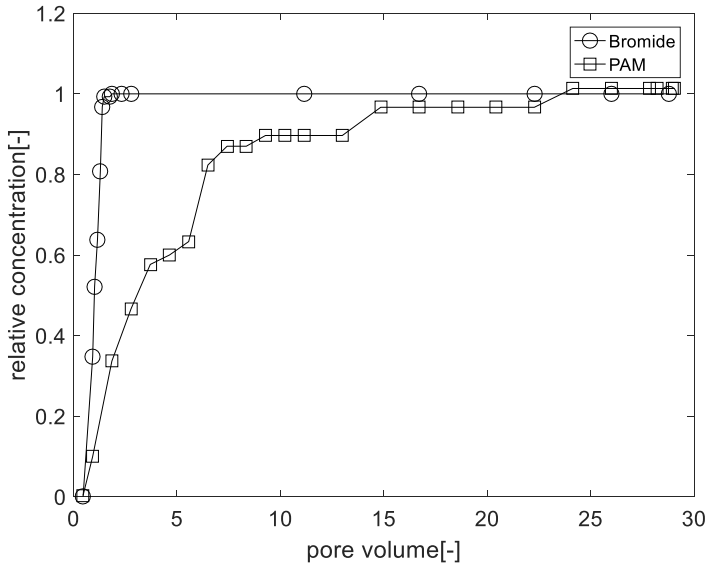

Figure 3.4. BTCs of Br^- and PAM at the pumping rate of 30 ml/min.

Figure 3.4 shows BTCs of Br^- and PAM at flow rate of 30 ml/min. As expected, PAM traveled much slower than Br^- in the soil. The concentration of Bromide quickly increased to the input concentration, while strong tailing behavior was observed in PAM's BTC. PAM's pore volume is approximately ten times as that of bromide to reach the equilibrium concentration. The position of PAM's BTC depends on the extent of sorption [20]. The right shift of PAM's BTC indicates strong soil sorption of PAM. An advection-diffusion model with a parameterization of sorption process should be used to describe the dynamics of PAM migration. Symmetry and sigmoid curve of bromide's BTC suggests absence of physical nonequilibrium. A two-region (mobile-immobile) model which is developed for physical nonequilibrium may not be needed [21].

Figure 3.5 shows simulated and observed BTCs of PAM at different flow rates.

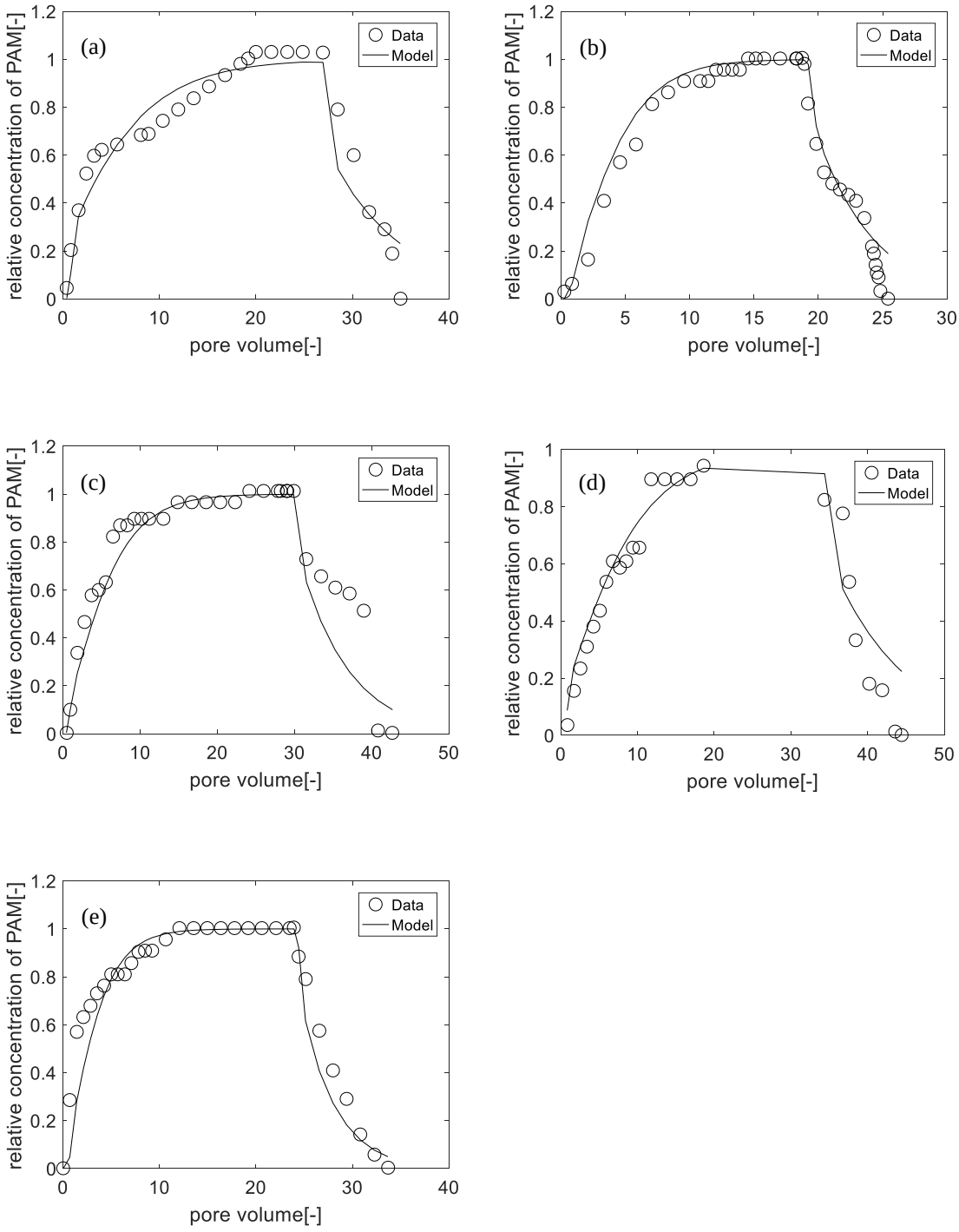

Figure 3.5. Experimental measurements and model predictions of PAM at flow rates of (a) $Q = 10ml/\min$ (b) $Q = 20ml/\min$ (c) $Q = 30ml/\min$ (d) $Q = 40ml/\min$ (e) $Q = 50ml/\min$. Circles are experimental measurements. .

It can be seen from Figure 3.5 that the one-site Langmuir model simulations agree closely with observations. Initially, we tried to fit a model with the instantaneous equilibrium assumption to experiment data of PAM but it failed to describe BTCs of PAM, even at a low pore velocity. The failure of models with the equilibrium sorption assumption is consistent with previous research of modeling nonequilibrium contaminant transport in the subsurface [20][22][23]. Because the experimental BTC of PAM was asymmetrical, which cannot be described by equilibrium models [22][24].

Asymmetrical BTCs could be caused by the sorption-related non-equilibrium, non-linear isotherm, and non-single-value sorption-desorption [20]. As shown in figure 3.4, the absence of physical non-equilibrium is confirmed by symmetrical and sigmoidal bromide's BTCs. and sorption-related process is the main cause of non-equilibrium of PAM. the static sorption of PAMs was well described by a non-linear single value isotherm Langmuir isotherm. Thus, in our column studies, both sorption-related non-equilibrium and non-linear isotherm may contribute to asymmetrical BTCs of PAMs. The non-equilibrium transport model we developed, Eqs. (2.3)-(2.5), incorporates a non-linear isotherm and describes non-equilibrium sorption by a Langmuir mass transfer [25][26].

Non-linear isotherm leads to non-coincident front and back curves [20] . Therefore, the effect of non-linear can be illustrated by comparison of front and back curves. Figure 3.6 showing large discrepancy between front and back portions of PAM's BTCs suggests that the sorption behavior may be affected by flow rates due to the effect of the non-linear isotherm varying with flow rates. The traditional first-order nonequilibrium mass transfer model with a linear sorption isotherm can only yield symmetric front and back BTCs.

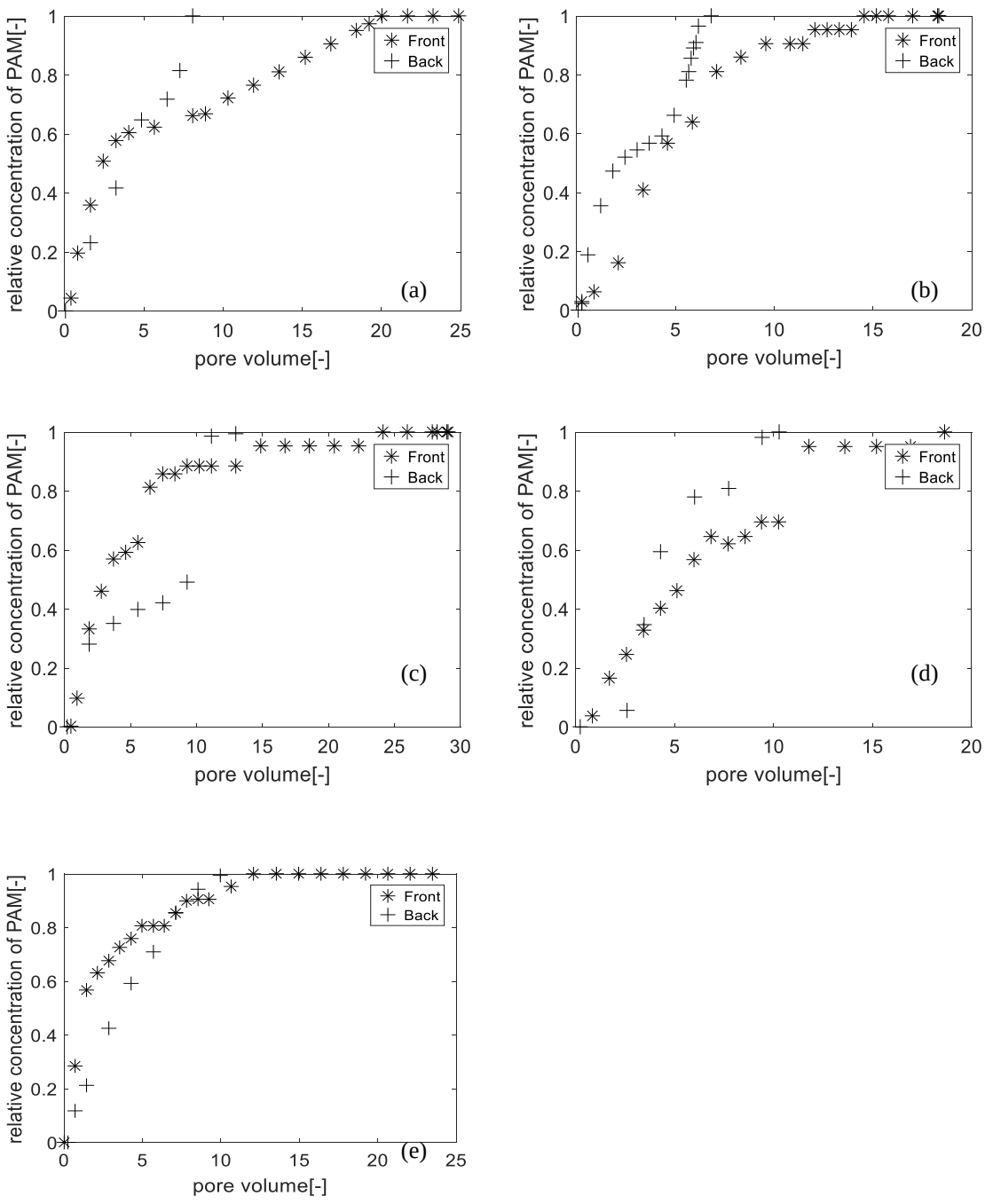

Figure 3.6. Comparison of front and back curves at flow rates of (a) $Q = 10ml/\min$ (b) $Q = 20ml/\min$ (c) $Q = 30ml/\min$ (d) $Q = 40ml/\min$ (e) $Q = 50ml/\min$.

3.4 Comparison with Linear Isotherm

At low concentrations a Langmuir isotherm may be simplified into a linear isotherm, the most commonly used sorption model of nonequilibrium transport. The first-order linear mass transfer equation is:

$$\rho \frac{\partial S}{\partial t} = \alpha (K_d C - S) \tag{3.2}$$

Langmuir mass transfer equation Eq.(2.5) can be simplified into following equation , which is similar to Eq. (3.2), when equilibrium concentration is small enough.

$$\rho \frac{\partial S}{\partial t} = \alpha (\Gamma_{\max} K_L C - S) \tag{3.3}$$

The asymmetric sorption and desorption behavior discussed in the previous section indicates that the PAM transport cannot be described by the linear sorption model for symmetric sorption and desorption. Figure 3.7 further illustrates the discrepancy between these two models for PAM transport at different concentrations.

As discussed above, transport of PAMs at low equilibrium concentration of PAMs is well described by the linear mass transfer model. In Figure 3.7a, the equilibrium concentration is within the linear stage of static Langmuir isotherm. Hence, both Langmuir and linear model are applicable to predicting PAM's concentration and the two models produce identical results. However, the sorption process becomes more non-linear with increasing equilibrium concentration. As shown in Figure 3.7b and Figure 3.7c, discrepancy between two models is large for equilibrium concentration of PAM was 300 mg/L or 600 mg/L.

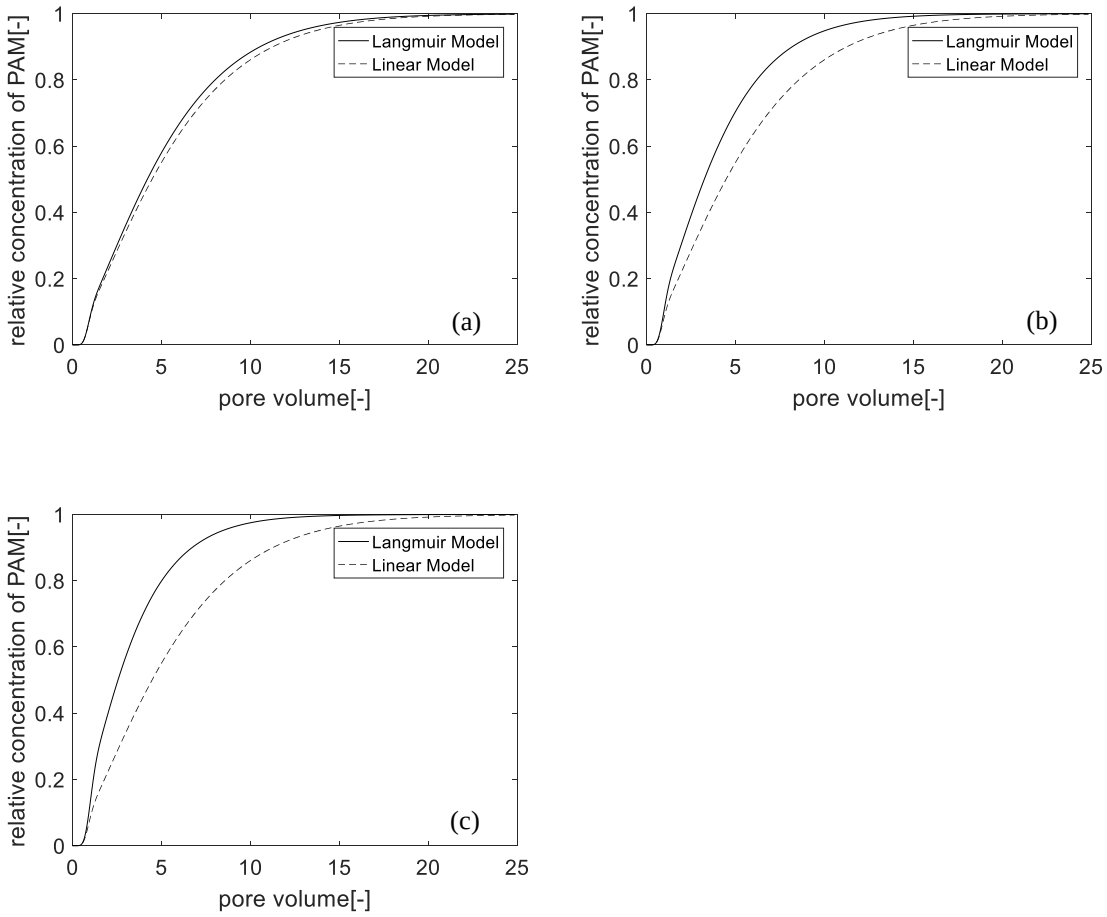

Figure 3.7. Discrepancy between nonequilibrium transport models with sorption isotherms described by a Langmuir model and a linear model. Values of input parameters are determined based on experimental data of nonequilibrium sorption of PAM and identical for both Langmuir and linear models. The equilibrium concentration is 50 mg/L, 300 mg/L and 600 mg/L for (a), (b) and (c).

3.5 Correlation with Flow Velocity

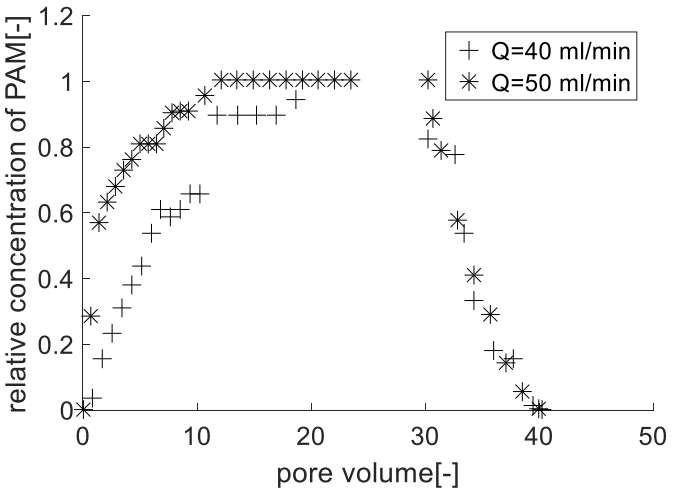

Figure 3.8. Comparison of BTCs at Different Velocities

Table 3.2. Parameters in the One-site Nonequilibrium Model

v (cm/min)	D_H (cm^2/min)	Q (ml/min)	θ	K (L/mg)	Cr (mg/mg)	α (10^4·mg/(L·min))
0.538	0.242	10	0.237	0.0016	0.08	0.0165
0.828	0.242	20	0.308	0.0016	0.08	0.0497
1.856	0.834	30	0.206	0.0016	0.08	0.0741
2.278	1.025	40	0.224	0.0016	0.08	0.0888
2.372	1.068	50	0.268	0.0016	0.08	0.1074

Figure 3.8 shows the BTCs at two velocities, demonstrating a shift of the sorption process but similar desorption processes. Both similarity and shift of BTCs absorbing chemicals were observed in earlier studies. Brusseau et al.(1991) and Lee et al.(1988) [27][28] reported left shift with higher velocities for organic chemicals. Brusseau (1992) [21] also observed similarity of BTCs at different velocities in low organic-carbon content soil.

Table 3.2 summaries fitted parameters in our model. Among these parameters, pore velocity v and dispersion coefficient D_H were estimated from BCTs of Br^-. Langmuir constant K and Cr were estimated from the static sorption of PAM. Only mass transfer rate coefficients α were estimated using the BTCs.

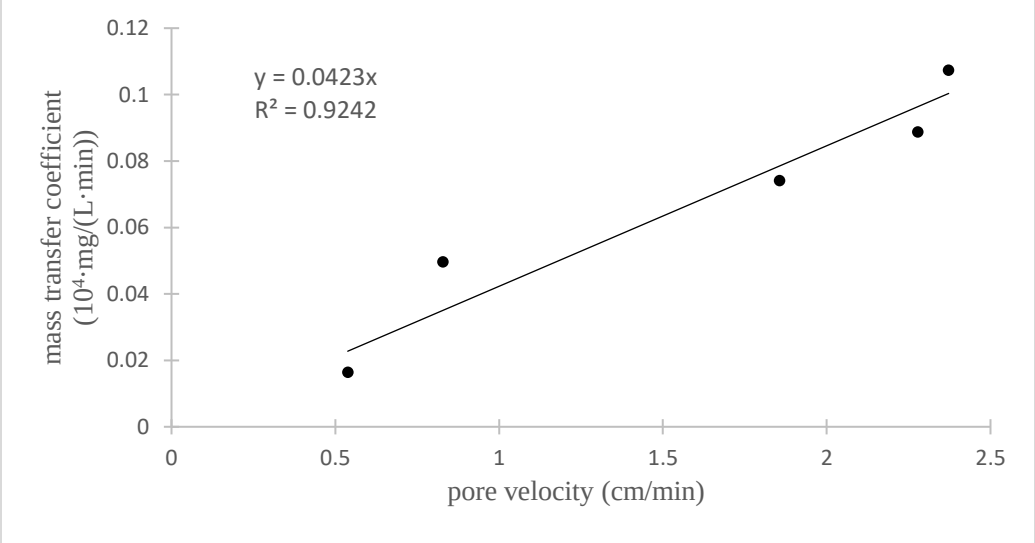

Figure 3.9. Relationship between pore velocity and mass transfer rate coefficient

Figure 3.9 displays the estimated mass transfer rate coefficient vs. pore velocity, which clearly shows a linear relationship between α and v. Velocity dependent mass transfer coefficient in a two-site non-equilibrium model was observed by numerous earlier studies [21][23][29][30]. Maraqa (2008) obtained the best-fit equation $\alpha = 0.095v^{0.97}$ with R^2 of 0.61

[29]. Kookana and Schuller [23] obtained a similar equation with R^2 of 0.566. Contaminants studied previously included organic matter, inorganic iron, pesticides and herbicides except for polymers. Our results show that linear relationship between pore velocity and mass transfer rate coefficients also holds for PAM, which will be used for upscaling subsurface transport models.

Rao et.al (1980) [31] found that mass transfer coefficient increases with pore velocity for physical non-equilibrium since mass transfer coefficient increases with velocity and reduces the traveling time of chemicals into immobile domains [21]. This mechanism also explains the linear relationship observed in the sorption-related non-equilibrium transport. In addition to velocity, mass transfer coefficient also depends on other parameters including input concentrations of solutes and aggregate sizes [23].

CHAPTER 4. CONCLUSION

Both experimental and modeling studies were conducted to investigate the subsurface transport behavior of PAMs at high concentrations. Pore-scale velocities and dispersion coefficients were obtained by fitting advection-diffusion models to concentration curves of tracer Br^-. A Langmuir isotherm was determined based on the static equilibrium sorption experiment of PAMs. In the flow-through column experiment, nonequilibrium sorption behavior of PAMs was well described by a one-site nonequilibrium mass transfer model combined with the Langmuir sorption model. Comparing with the traditional nonequilibrium mass transfer model with a linear isotherm, the developed nonlinear model predicts asymmetric sorption and desorption behavior. A linear relationship between the mass transfer rate coefficient and pore velocity was established using experimental data. This study is limited to one type of soil under the condition of constant temperature and ionic strength. We have demonstrated that mass transfer is a limiting factor for subsurface PAMs transport and the lumped mass transfer rate coefficients are flow velocity dependent.

APPENDIX A. CODE OF PROGRAM

```
clear;


% Data
tBr=[3,7.5,10.5,12,12.75,13.5,14.25,15,16.5];
C_Br=[0,0,5,19,82,102,110,114,114];


% Parameters
c0_Br = 120; % mg/L


q = 0.255; % cm/min
L = 10; % cm, measurment location


 % Initial guess
 por0 = 0.45;
D0 = 10; % cm^2/min
X0=[por0 D0];
% Fitting
option = optimset('display','iter');
X = fminsearch(@fitDlinear,X0,option,q, L, c0_Br,tBr, C_Br);
D=abs(X(2));
por=abs(X(1));      % groundwater velocity --> average linear gw velocity
DHP=D/por;   % hydrodynamic disp. coef. = alfa * V
V=q/por;
```

```
cbound=c0_Br; % concentration at boundary on left
tspan = linspace(max(tBr)/100,tBr(end));

cmodel = cbound/2*(erfc((L-V*tspan)/2./sqrt(DHP*tspan))+exp(V*L/DHP)*erfc((L+V*tspan)/2./sqrt(DHP*tspan)));
cmodel = [0 cmodel];

% Plotting
figure
plot(tBr, C_Br, 'ko', [0 tspan], cmodel,'k-');
xlabel('Time [min]'); ylabel('C_{Br} [mg/L]');



function MSE = fitDlinear(X,q,L, c0_Br, tBr, C_Br)

D=abs(X(2));
por=abs(X(1));      % groundwater velocity --> average linear gw velocity
V=q/por;% hydrodynamic disp. coef. = alfa * V
DHP=D/por;
cbound=c0_Br; % concentration at boundary on left
tspan = tBr(2:end);

% ct = cbound/2*(erfc((L-V*tspan)/2./sqrt(DHP*tspan))+exp(V*L/DHP)*erfc((L+V*tspan)/2./sqrt(DHP*tspan)));
ct = cbound/2*(erfc((L-V*tspan)/2./sqrt(DHP*tspan)));
ct = [0 ct];
```

```
% time and space markers for concentration histories

MSE = sum((ct-C_Br).^2);

clear;
global cmodel;
global tBr;
global C_Br;
global Kb;
global Kf;
global cmodelfull;
global t;

% Data
tBr=[1,3.3,6.3,9.3,12.3];
C_Br=[127.7,99.6,55.3,29.8,0];
% Parameters
Kb=0;
Kf=0;
 % Initial guess
v0 = 0.01; % cm^2/hr
DHP0 = 0.01 ;

X0=[v0,DHP0];
```

```
% Fitting
t=0:0.1:60;
X = fminsearch(@FitBr2,X0);
figure
plot(tBr, C_Br, 'ko', t, cmodelfull,'k-');
xlabel('Time [min]'); ylabel('C_{Br} [mg/L]');

function MSE = FitBr2(X)

global v;
global Kb;
global Kf;
global DHP;
global tBr;
global C_Br;
global cmodel;
global cmodelfull;
global t;
v=X(1);
DHP=X(2);
m=0;
x=0:1:20;
sol=pdepe(m,@pdefunBr,@pdeicBr,@pdebcBr,x,t);
cmodelfull=sol(:,11,1);
cmodel=sol(round(tBr*10),11,1);
```

```
MSE = sum((transpose(cmodel)-C_Br).^2);


function[pa,qa,pb,qb]=pdebcBr(xa,ua,xb,ub,t) % boundary condition

pa=[ua(1);0];

qa=[0;1];

pb=[ub(1);0];

qb=[0;1];


function[c,f,s]=pdefunBr(x,t,u,DuDx)

global Kb;

global Kf;

global v;

global DHP;

c=[1;1];

f=[DHP*DuDx(1);0];

s=[-v*DuDx(1)+u(2)*Kf-Kb*u(1);u(1)*Kb-u(2)*Kf];


function u0=pdeicBr(x) %initial condition


u0=[120;0.00]


% Data

tPAM=[2.5,5,10,15,20,25,30,35,40,45,50,55,60,70,80,90,100,110,120,130,140,150,152,1
56,156.5];

C_PAM=[1,30,101,140,173,180,190,247,261,261,269,269,269,269,290,290,290,290,290,
304,304,304,304,304,304];
```

```
% Parameters
q=0.38;
D=0.1032;
por=0.211;
 % Initial guess
Kf0 = 0.01; % cm^2/hr
Kb0 = 0.01 ;
BD0=1;
X0=[Kb0,Kf0,BD0];

% Fitting
t=0:0.1:250;
X = fminsearch(@Fitkinetic2,X0);
figure
plot(tPAM, C_PAM, 'ko', tPAM, cmodel,'k-');
xlabel('Time [min]'); ylabel('C_{PAM} [mg/L]');



function MSE = Fitkinetic2(X)

global q;
```

```
global Kb;
global Kf;
global D;
global tPAM;
global C_PAM;
global cmodel;
global t;
global BD;
Kb=abs(X(1));
Kf=abs(X(2));
BD=abs(X(3));
m=0;
x=0:1:20;

sol=pdepe(m,@pdefun,@pdeic,@pdebc,x,t);
cmodel=sol(round(tPAM*10),11,1);
MSE = sum((transpose(cmodel)-C_PAM).^2);

function[pa,qa,pb,qb]=pdebc(xa,ua,xb,ub,t) % boundary condition
pa=[ua(1)-300;0];
qa=[0;1];
pb=[ub(1);0];
qb=[0;1];

function[c,f,s]=pdefun(x,t,u,DuDx)
```

```
global Kb;
global Kf;
global q;
global D;
global por;
global BD;
c=[por;BD];
f=[D*DuDx(1);0];
s=[-q*DuDx(1)+u(2)*Kf-Kb*u(1);u(1)*Kb-u(2)*Kf];

function u0=pdeic(x) %initial condition

u0=[31.43;0.00]

clear;
global cmodel;
global tPAM;
global C_PAM;
global Kb;
global Kf;
global cmodelfull;
global t;
global sol;
global por;
global Kf1;
```

```
global Kb1;
global a;
global vmin;
% Data
tPAM=[1,3,6,12,18,24,30,36,42];
C_PAM=[301.4,265.7,237.1,172.9,122.9,87.1,42.9,17.1,1.43];



% Parameters
Kb1=0.0092;
Kf1=0.0299;
vmin=0.64;
 % Initial guess
Kb0=0.01;
Kf0=0.01;
v0=0.17;
DHP0=0.1175;
BD0=1;
a=0.041/0.0148;
X0=[Kb0,Kf0,v0,DHP0,BD0];

% Fitting
t=0:0.1:100;
X = fminsearch(@FitPAM2,X0);
```

```
figure
plot(tPAM, C_PAM, 'ko', t, cmodelfull,'k-');
xlabel('Time [min]'); ylabel('C_{PAM} [mg/L]');

function MSE = FitPAM2(X)

global v;
global Kb;
global Kf;
global DHP;
global tPAM;
global C_PAM;
global cmodel;
global cmodelfull;
global t;
global a;
global sol;
global BD;
global vmin;
Kb=abs(X(1));
Kf=abs(X(2));
v=abs(X(3))+vmin;
DHP=abs(X(4));
BD=abs(X(5));
m=0;
```

```
x=0:1:20;
sol=pdepe(m,@pdefunPAM,@pdeicPAM,@pdebcPAM,x,t);
cmodelfull=sol(:,11,1);
cmodel=sol(round(tPAM*10),11,1);
MSE = sum((transpose(cmodel)-C_PAM).^2);

function[pa,qa,pb,qb]=pdebcPAM(xa,ua,xb,ub,t) % boundary condition
pa=[ua(1);0];
qa=[0;1];
pb=[ub(1);0];
qb=[0;1];

function[c,f,s]=pdefunPAM(x,t,u,DuDx)
global Kb;
global Kf;
global v;
global DHP;
global BD;
global por;
c=[1;BD];
f=[DHP*DuDx(1);0];
s=[-v*DuDx(1)+u(2)*Kf-Kb*u(1);u(1)*Kb-u(2)*Kf];

function u0=pdeicPAM(x) %initial condition
global Kb1;
```

```
global Kf1;
global a;
u0=[300;300*a]
```

REFERENCES

[1] Wen, Qinxue, et al. "Biodegradation of polyacrylamide by bacteria isolated from activated sludge and oil-contaminated soil." Journal of hazardouss materials 175.1 (2010): 955-959.

[2] Sojka, R. E., et al. "Polyacrylamide in agriculture and environmental land management." Advances in Agronomy 92 (2007): 75-162.

[3] Sojka R E, Entry J A, Fuhrmann J J. The influence of high application rates of polyacrylamide on microbial metabolic potential in an agricultural soil[J]. Applied Soil Ecology, 2006, 32(2): 243-252.

[4] Lu J H, Wu L, Letey J. Effects of soil and water properties on anionic polyacrylamide sorption[J]. Soil Science Society of America Journal, 2002, 66(2): 578-584.

[5] Ben-Hur M, Malik M, Letey J, et al. Adsorption of polymers on clays as affected by clay charge and structure, polymer properties, and water quality[J]. Soil Science, 1992, 153(5): 349-356.

[6] Asghari S, Abbasi F, Neyshabouri M R. Effects of soil conditioners on physical quality and bromide transport properties in a sandy loam soil[J]. Biosystems engineering, 2011, 109(1): 90-97.

[7] Ver Vers, Leonard M. "Determination of acrylamide monomer in polyacrylamide degradation studies by high-performance liquid chromatography." Journal of chromatographic science 37.12 (1999): 486-494.

[8] Ho Y C, Norli I, Alkarkhi A F M, et al. Characterization of biopolymeric flocculant (pectin) and organic synthetic flocculant (PAM): a comparative study on treatment and optimization in kaolin suspension[J]. Bioresource technology, 2010, 101(4): 1166-1174.

[9] Meadows J, Williams P A, Garvey M J, et al. Characterization of the adsorption—desorption behavior of hydrolyzed polyacrylamide[J]. Journal of Colloid and Interface Science, 1989, 132(2): 319-328.

[10] Malik, M., and J. Letey. "Adsorption of polyacrylamide and polysaccharide polymers on soil materials." Soil Science Society of America Journal 55.2 (1991): 380-383.

[11] Giles C H, Smith D, Huitson A. A general treatment and classification of the solute adsorption isotherm. I. Theoretical[J]. Journal of Colloid and Interface Science, 1974, 47(3): 755-765.

[12] Nabzar L, Pefferkorn E, Varoqui R. Stability of polymer—clay suspensions. The polyacrylamide—sodium kaolinite system[J]. Colloids and surfaces, 1988, 30(2): 345-353.

[13] Aggelopoulos C A, Tsakiroglou C D. The longitudinal dispersion coefficient of soils as related to the variability of local permeability[J]. Water, air, and soil pollution, 2007, 185(1-4): 223-237.

[14] Theng B K G. Clay–polymer interactions: summary and perspectives[C]//Clays and Clay Minerals. 1982.

[15] Walter M T, Gao B, Parlange J Y. Modeling soil solute release into runoff with infiltration[J]. Journal of hydrology, 2007, 347(3): 430-437.

[16] Magga Z, Tzovolou D N, Theodoropoulou M A, et al. Soil column experiments used as a means to assess transport, sorption, and biodegradation of pesticides in groundwater[J]. Journal of Environmental Science and Health Part B, 2008, 43(8): 732-741.

[17] Schulze‐Makuch, Dirk. "Longitudinal dispersivity data and implications for scaling behavior." Ground Water 43.3 (2005): 443-456.

[18] Coats K H, Smith B D. Dead-end pore volume and dispersion in porous media[J]. Society of petroleum engineers journal, 1964, 4(01): 73-84.

[19] Hendry M J, Lawrence J R, Maloszewski P. Effects of velocity on the transport of two bacteria through saturated sand[J]. Ground Water, 1999, 37(1): 103-112.

[20] Brusseau M L, Rao P S C, Gillham R W. Sorption nonideality during organic contaminant transport in porous media[J]. Critical Reviews in Environmental Science and Technology, 1989, 19(1): 33-99.

[21] Brusseau M L. Nonequilibrium transport of organic chemicals: The impact of pore-water velocity[J]. Journal of Contaminant Hydrology, 1992, 9(4): 353-368.

[22] Baskaran S, Bolan N S, Rahman A, et al. Non-equilibrium sorption during the movement of pesticides in soils[J]. Pesticide science, 1996, 46(4): 333-343.

[23] Kookana, Rai S., R. D. Schuller, and L. A. G. Aylmore. "Simulation of simazine transport through soil columns using time-dependent sorption data measured under flow conditions." Journal of contaminant hydrology 14.2 (1993): 93-115.

[24] Davidson J M, Rieck C E, Santelmann P W. Influence of water flux and porous material on the movement of selected herbicides[J]. Soil Science Society of America Journal, 1968, 32(5): 629-633.

[25] Harvey C F, Haggerty R, Gorelick S M. Aquifer remediation: A method for estimating mass transfer rate coefficients and an evaluation of pulsed pumping[J]. Water Resources Research, 1994, 30(7): 1979-1991.

[26] Sardin M, Schweich D, Leij F J, et al. Modeling the nonequilibrium transport of linearly interacting solutes in porous media: A review[J]. Water Resources Research, 1991, 27(9): 2287-2307.

[27] Brusseau, Mark L., Ron E. Jessup, and P. SC Rao. "Nonequilibrium sorption of organic chemicals: elucidation of rate-limiting processes." Environmental Science and Technology 25.1 (1991): 134-142.

[28] Lee, L. S., et al. "Nonequilibrium sorption of organic contaminants during flow through columns of aquifer materials." Environmental Toxicology and Chemistry 7.10 (1988): 779-793.

[29] Maraqa M A. Prediction of mass-transfer coefficient for solute transport in porous media[J]. Journal of contaminant hydrology, 2001, 50(1): 1-19.

[30] Vereecken H, Vanderborght J, Kasteel R, et al. Do lab-derived distribution coefficient values of pesticides match distribution coefficient values determined from column and field-scale experiments? A critical analysis of relevant literature[J]. Journal of environmental quality, 2011, 40(3): 879-898.

[31] Rao, P. S. C., et al. "Experimental and mathematical description of nonadsorbed solute transfer by diffusion in spherical aggregates." Soil Science Society of America Journal 44.4 (1980): 684-688.